Cell Metabolism
Article

Total Skeletal Muscle PGC-1 Deficiency Uncouples Mitochondrial Derangements from Fiber Type Determination and Insulin Sensitivity

Christoph Zechner,[1,3,6] Ling Lai,[1,3] Juliet F. Zechner,[1,3,6] Tuoyu Geng,[4,5] Zhen Yan,[4,5] John W. Rumsey,[3] Deanna Collia,[3] Zhouji Chen,[1] David F. Wozniak,[2] Teresa C. Leone,[1,3] and Daniel P. Kelly[1,3,*]
[1]Department of Medicine
[2]Department of Psychiatry
Washington University School of Medicine, St. Louis, MO 63110, USA
[3]Sanford-Burnham Medical Research Institute, Orlando, FL 32827, USA
[4]Department of Medicine
[5]Center for Skeletal Muscle Research at Robert M. Berne Cardiovascular Research Center
University of Virginia School of Medicine, Charlottesville, VA, 22908, USA
[6]Present address: Department of Internal Medicine, University of Texas Southwestern Medical Center, Dallas, TX 75390, USA
*Correspondence: dkelly@sanfordburnham.org
DOI 10.1016/j.cmet.2010.11.008

SUMMARY

Evidence is emerging that the PGC-1 coactivators serve a critical role in skeletal muscle metabolism, function, and disease. Mice with total PGC-1 deficiency in skeletal muscle (PGC-1$\alpha^{-/-}\beta^{f/f/MLC\text{-}Cre}$ mice) were generated and characterized. PGC-1$\alpha^{-/-}\beta^{f/f/MLC\text{-}Cre}$ mice exhibit a dramatic reduction in exercise performance compared to single PGC-1α- or PGC-1β-deficient mice and wild-type controls. The exercise phenotype of the PGC-1$\alpha^{-/-}\beta^{f/f/MLC\text{-}Cre}$ mice was associated with a marked diminution in muscle oxidative capacity, together with rapid depletion of muscle glycogen stores. In addition, the PGC-1α/β-deficient muscle exhibited mitochondrial structural derangements consistent with fusion/fission and biogenic defects. Surprisingly, the proportion of oxidative muscle fiber types (I, IIa) was not reduced in the PGC-1$\alpha^{-/-}\beta^{f/f/MLC\text{-}Cre}$ mice. Moreover, insulin sensitivity and glucose tolerance were not altered in the PGC-1$\alpha^{-/-}\beta^{f/f/MLC\text{-}Cre}$ mice. Taken together, we conclude that PGC-1 coactivators are necessary for the oxidative and mitochondrial programs of skeletal muscle but are dispensable for fundamental fiber type determination and insulin sensitivity.

INTRODUCTION

The transcriptional coactivators PPARγ coactivator-1α (PGC-1α) and PGC-1β serve as regulators of mitochondrial biogenesis and cellular energy metabolism (Kelly and Scarpulla, 2004; Lin et al., 2005). Originally discovered in brown adipose tissue (Puigserver et al., 1998), PGC-1α enhances transcription by interacting directly with target transcription factors, including PPARγ and other members of the nuclear receptor superfamily (reviewed in Finck and Kelly, 2006; Handschin and Spiegelman, 2006). The PGC-1 coactivators are enriched in tissues with high capacity for mitochondrial respiratory function, such as brown adipose tissue, heart, and skeletal muscle, and are highly inducible in response to physiological stimuli, including exercise, fasting, and cold exposure (Wu et al., 1999; Goto et al., 2000; Lehman et al., 2000; Baar et al., 2002; Pilegaard et al., 2003; Finck and Kelly, 2006).

Evidence is emerging that PGC-1 signaling plays an important role in skeletal muscle structure and function (Lin et al., 2002a; Arany et al., 2005, 2007; Leone et al., 2005; Lelliott et al., 2006; Handschin et al., 2007). Tissue-specific transgenic approaches in mice have shown that forced overexpression of PGC-1 coactivators in skeletal muscle increases muscle oxidative capacity and the proportions of type I and IIa fibers (Lin et al., 2002a). PGC-1β has been shown to drive formation of type IIx fibers (Arany et al., 2007). Using a skeletal-muscle-specific, doxycycline-regulated system, we found that acute induction of PGC-1α expression in mice increased muscle glycogen stores, a signature of training (Wende et al., 2007). Collectively, the results of the forced expression studies suggest that induction of PGC-1α, which is known to occur following exercise, drives a trained skeletal muscle phenotype. However, gain-of-function studies have not defined the role of PGC-1 coactivators in fundamental skeletal muscle development, fiber type specification, or mitochondrial biogenesis. Insights gained from PGC-1 coactivator mouse "knockout" studies to date have been limited due to the functionally redundant actions of PGC-1α and PGC-1β; single PGC-1 gene deletion lines exhibit relatively minimal phenotypes (Lin et al., 2004; Leone et al., 2005; Lelliott et al., 2006; Vianna et al., 2006; Sonoda et al., 2007). Mice with generalized combined deficiency of PGC-1α and PGC-1β (PGC-1$\alpha\beta^{-/-}$ mice) die of severe heart failure shortly after birth, precluding evaluation of the skeletal muscle phenotype in this model (Lai et al., 2008).

Recently, dysregulation of PGC-1 coactivators has been implicated in the development of skeletal muscle insulin resistance (Mootha et al., 2003; Patti et al., 2003), although this notion is controversial. Single PGC-1α or PGC-1β "knockout" mouse

models have generally not demonstrated insulin-resistant or glucose-intolerant phenotypes (Lin et al., 2004; Leone et al., 2005; Lelliott et al., 2006; Vianna et al., 2006; Sonoda et al., 2007). Again, the difficulty in interpreting these studies relates to the functional overlap between the PGC-1 coactivators, setting the stage for compensatory or even supercompensatory responses by the remaining coactivator.

Given the importance of PGC-1 coactivators in muscle biology and their potential role in the metabolic basis of disease, we embarked on a study to define the necessary functions of these regulatory factors in skeletal muscle using a conditional loss-of-function strategy in mice. To this end, a gene-targeting approach was used to establish mice with skeletal-muscle-specific PGC-1β deficiency on a generalized PGC-1α-deficient background. We found that combined deficiency of PGC-1α and PGC-1β in skeletal muscle results in a dramatic exercise performance phenotype related to mitochondrial structural and functional abnormalities. Surprisingly, PGC-1$\alpha^{-/-}\beta^{f/f/MLC\text{-}Cre}$ mice did not exhibit a defect in fundamental muscle fiber type formation or abnormalities in glucose tolerance or insulin sensitivity.

RESULTS

Dramatic Exercise Deficit in Mice with Muscle PGC-1α/β Deficiency

The *PGC-1β* gene was disrupted via *loxP*-mediated excision in skeletal muscle by Cre recombinase (Cre) expressed under the control of the myosin light chain 1f (MLC1f) promoter (PGC-$1\beta^{f/f/MLC\text{-}Cre}$ mice) (Figure S1A). Consistent with the type II fiber specificity of the MLC-1f promoter (Donoghue et al., 1991; Parsons et al., 2004), *PGC-1β* gene expression was markedly reduced in gastrocnemius (GC) (residual levels 10.9% ± 1.3% of PGC-$1\beta^{f/f}$) and white vastus (9.0% ± 1.5% of PGC-$1\beta^{f/f}$) muscles of PGC-$1\beta^{f/f/MLC\text{-}Cre}$ mice, but to a lesser extent in soleus muscle (44% ± 8.5% of PGC-$1\beta^{f/f}$) (Figure S1B), which contains a greater proportion of type I fibers. Immunoblotting studies confirmed that PGC-1β protein levels were undetectable in primary cells derived from GC muscle of PGC-$1\alpha^{-/-}\beta^{f/f/MLC\text{-}Cre}$ mice (Figure S1C). *PGC-1β* gene expression was not reduced in heart or liver in the PGC-$1\beta^{f/f/MLC\text{-}Cre}$ mice (Figure S1B). PGC-1α mRNA levels were unchanged in the muscle of the PGC-$1\beta^{f/f/MLC\text{-}Cre}$ mice (data not shown). PGC-$1\beta^{f/f/MLC\text{-}Cre}$ mice survived, appeared normal compared to WT littermates, and did not exhibit overt abnormalities in locomotor activity. To generate lines with skeletal muscle deficiency of both PGC-1α and PGC-1β, the PGC-$1\beta^{f/f/MLC\text{-}Cre}$ mice were crossed into a generalized PGC-$1\alpha^{-/-}$ background (Leone et al., 2005), a strategy that was used previously to generate mice with combined deficiency of PGC-1α and PGC-1β in heart (Lai et al., 2008). Mice with combined PGC-1α and PGC-1β deficiency in skeletal muscle (PGC-$1\alpha^{-/-}\beta^{f/f/MLC\text{-}Cre}$ mice) were viable, appeared normal on inspection, and did not exhibit any overt abnormalities in locomotor activity. Fasting circulating triglyceride and glucose levels were not abnormal in the PGC-$1\alpha^{-/-}\beta^{f/f/MLC\text{-}Cre}$ mice (data not shown).

We and others have shown that PGC-1α-deficient mice exhibit a mild exercise performance phenotype (Leone et al., 2005; Handschin et al., 2007; Lai et al., 2008). To define the impact of muscle-specific PGC-1β deficiency and combined PGC-1α/PGC-1β deficiency on exercise performance, the PGC-$1\beta^{f/f/MLC\text{-}Cre}$ and PGC-$1\alpha^{-/-}\beta^{f/f/MLC\text{-}Cre}$ mice were subjected to a low-intensity run-to-exhaustion protocol on a motorized treadmill. Compared to the performance of "floxed" controls (170.2 ± 7.1 min), PGC-$1\alpha^{-/-}\beta^{f/f}$ and PGC-$1\beta^{f/f/MLC\text{-}Cre}$ mice demonstrated a mild but significant performance deficit (mean running times of 114 ± 7.1 min and 140 ± 8.8 min, respectively) (Figure 1). In striking contrast, PGC-$1\alpha^{-/-}\beta^{f/f/MLC\text{-}Cre}$ mice exhibited a dramatic exercise phenotype, showing exhaustion after an average of only 6.6 ± 1.6 min (Figure 1).

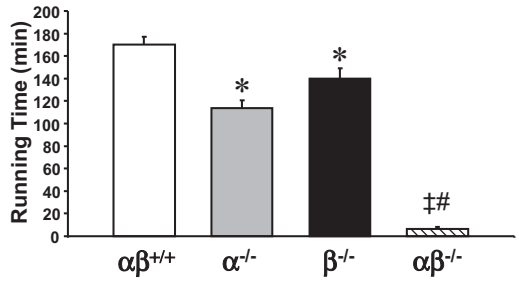

Figure 1. Global Loss of PGC-1α Combined with Muscle-Specific Loss of PGC-1β Results in a Dramatic Exercise Performance Deficit

Two- to three-month-old male PGC-$1\beta^{f/f}$ ($\alpha\beta^{+/+}$), PGC-$1\alpha^{-/-}\beta^{f/f}$ ($\alpha^{-/-}$), PGC-$1\beta^{f/f/MLC\text{-}Cre}$ ($\beta^{-/-}$), and PGC-$1\alpha^{-/-}\beta^{f/f/MLC\text{-}Cre}$ ($\alpha\beta^{-/-}$) mice were subjected to a run-to-exhaustion protocol on a motorized treadmill (n = 6–7) as described in Experimental Procedures. Bars represent mean running time (± SEM) in minutes. *$p < 0.05$ versus $\alpha\beta^{+/+}$; ‡$p < 0.05$ versus $\alpha^{-/-}$; #$p < 0.05$ versus $\beta^{-/-}$. See also Figure S1.

Histological assessment of the GC muscle of PGC-$1\alpha^{-/-}\beta^{f/f/MLC\text{-}Cre}$ mice did not reveal any overt cellular derangements or fibrosis (Figure S1D and data not shown). However, a very slight increase in the proportion of myocytes with centralized nuclei was noted in PGC-$1\alpha^{-/-}\beta^{f/f/MLC\text{-}Cre}$ muscle fibers, indicative of increased muscle fiber regeneration (Figure S1E). As a measure of muscle damage, circulating creatine kinase (CK) was assayed in PGC-$1\alpha^{-/-}\beta^{f/f/MLC\text{-}Cre}$ mice and controls 30 min following a bout of exercise (protocol described in Supplemental Experimental Procedures). Mean plasma CK levels were mildly but significantly elevated in PGC-$1\alpha^{-/-}\beta^{f/f/MLC\text{-}Cre}$ mice compared to the other groups ($\beta^{f/f}$, 24.0 ± 3.5 U/l; $\alpha^{-/-}\beta^{f/f}$, 23.5 ± 2.3 U/l; $\beta^{f/f/MLC\text{-}Cre}$, 31.1 ± 6.3 U/l; $\alpha^{-/-}\beta^{f/f/MLC\text{-}Cre}$, 103 ± 37.4 U/l; $p < 0.004$), possibly consistent with mild skeletal muscle injury. Taken together, these results are unlikely to account for the profound exercise performance deficit of the PGC-$1\alpha^{-/-}\beta^{f/f/MLC\text{-}Cre}$ line.

The exercise phenotype of the PGC-$1\alpha^{-/-}\beta^{f/f/MLC\text{-}Cre}$ mice prompted us to assess general ambulatory activity and other parameters that may influence ambulation and exercise performance. Using a 1 hr locomotor activity test, both PGC-$1\alpha^{-/-}\beta^{f/f}$ and PGC-$1\alpha^{-/-}\beta^{f/f/MLC\text{-}Cre}$ lines exhibited a similar, modest decrease in total ambulations (whole-body movements) compared to the PGC-$1\beta^{f/f}$ group (Figure S1F, left). Time spent in the central and peripheral zones of the test area, as a measure of exploratory behavior, was also recorded and analyzed. PGC-$1\alpha^{-/-}\beta^{f/f}$ and PGC-$1\alpha^{-/-}\beta^{f/f/MLC\text{-}Cre}$ mice traveled significantly shorter distances within the peripheral zone (Figure S1F, middle) and entered the center less frequently (Figure S1F, right) when

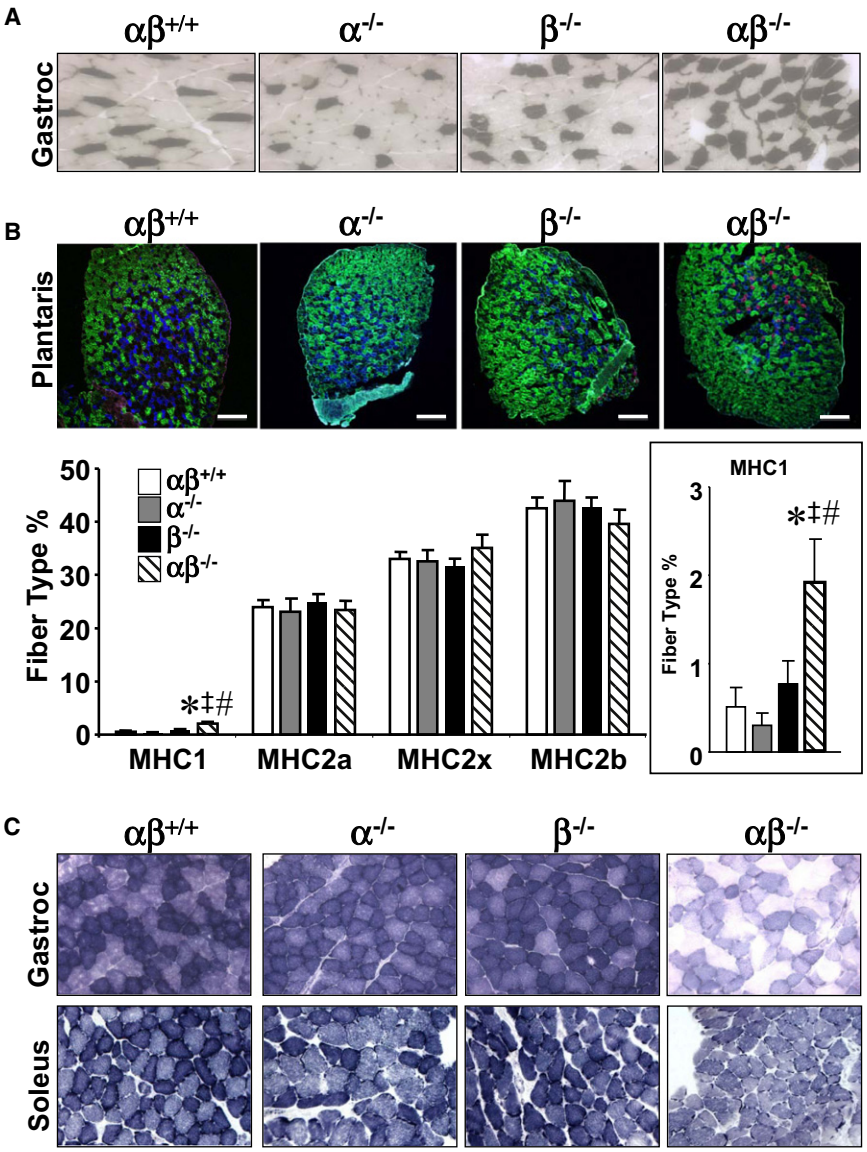

Figure 2. PGC-1$\alpha^{-/-}\beta^{f/f/MLC\text{-}Cre}$ Muscle Exhibits an Increase in MHC1-Positive Fibers without a Change in Type II Fiber Distribution

(A) Cross-sections of gastrocnemius (Gastroc) muscle of 3- to 6-month-old male PGC-1$\beta^{f/f}$ ($\alpha\beta^{+/+}$), PGC-1$\alpha^{-/-}\beta^{f/f}$ ($\alpha^{-/-}$), PGC-1$\beta^{f/f/MLC\text{-}Cre}$ ($\beta^{-/-}$), and PGC-1$\alpha^{-/-}\beta^{f/f/MLC\text{-}Cre}$ ($\alpha\beta^{-/-}$) mice (n = 5–6) stained for myosin I ATPase activity. Type I (MHC1-positive) fibers are stained dark. See also Figure S2.

(B) Top: Sections of plantaris muscle of 3- to 4-month-old male mice (n = 5–7) were immunostained for MHC1 (red), MHC2a (blue), and MHC2b (green). Representative images are shown. Scale bars denote 200 μm. Bottom: Quantification results of the plantaris muscle MHC immunostaining studies expressed as mean percent (± SEM) of total muscle fibers. Unstained muscle fibers were counted as MHC2x positive. Insert shows magnification of MHC1 results. *p < 0.05 versus $\alpha\beta^{+/+}$; ‡p < 0.05 versus $\alpha^{-/-}$; #p < 0.05 versus $\beta^{-/-}$.

(C) Succinate dehydrogenase (SDH) activity staining was performed on sections of gastrocnemius muscle (top row; n = 5–6) and soleus muscle (bottom row; n = 2) of 3- to 6-month-old male mice of the indicated genotypes.

compared to the PGC-1$\beta^{f/f}$ group. These collective results are consistent with our earlier findings that PGC-1α deficiency results in a mild decrease in general ambulatory activity and may induce emotional disturbances (Leone et al., 2005). However, this phenotype was not more severe in the PGC-1$\alpha^{-/-}\beta^{f/f/MLC\text{-}Cre}$ mice.

Interestingly, muscle strength, as assessed by forelimb grip studies, did not reveal differences between groups (Figure S1F, left). In addition, PGC-1$\alpha^{-/-}\beta^{f/f/MLC\text{-}Cre}$ mice did not differ from controls on ledge, platform (data not shown), or inverted screen tests (Figure S1G, right). Thus, PGC-1$\alpha^{-/-}\beta^{f/f/MLC\text{-}Cre}$ mice do not exhibit abnormalities in coordination, balance, or muscle strength beyond the phenotype that can be attributed to generalized PGC-1α deficiency.

PGC-1α/β Deficiency Uncouples Muscle Oxidative Capacity from Fiber Type Determination

To further evaluate the basis for the exercise phenotype in PGC-1$\alpha^{-/-}\beta^{f/f/MLC\text{-}Cre}$ mice, formal skeletal muscle fiber typing was conducted. First, fiber type distribution was examined in GC muscle using metachromatic ATPase staining under acidic conditions, which are permissive for myosin heavy chain 1 (MHC1) ATPase activity, but not for MHC2 ATPase. Surprisingly, analysis of the oxidative regions of GC muscle demonstrated a mild increase in numbers of MHC1-positive muscle fibers in PGC-1$\alpha^{-/-}\beta^{f/f/MLC\text{-}Cre}$ muscles compared to the other groups (Figure 2A).

We next performed quantitative immunohistochemical analyses of fiber type distribution in the muscle of the four genotypes. These studies were initially conducted on plantaris muscle, which exhibits less regional heterogeneity in oxidative fiber type compared with GC. Again, higher proportions of MHC1-positive fibers were noted in PGC-1$\alpha^{-/-}\beta^{f/f/MLC\text{-}Cre}$ muscle when compared with the other genotypes (Figure 2B). Moreover, type IIa, IIx, and IIb fiber proportions were not different among the groups (Figure 2B). Quantitative analysis of MHC mRNA transcripts in GC muscle of PGC-1$\alpha^{-/-}\beta^{f/f/MLC\text{-}Cre}$ mice revealed an increase in MHC1 mRNA levels in PGC-1$\alpha^{-/-}\beta^{f/f}$ and PGC-1$\alpha^{-/-}\beta^{f/f/MLC\text{-}Cre}$ mice and a modest but significant decrease in MHC2a and 2x mRNA levels in PGC-1$\alpha^{-/-}\beta^{f/f/MLC\text{-}Cre}$ muscle (Figure S2). These latter results suggest that posttranscriptional compensatory mechanisms may contribute to the maintenance of normal type II fiber distribution in the muscle of PGC-1$\alpha^{-/-}\beta^{f/f/MLC\text{-}Cre}$ mice.

We next assessed the oxidative capacity of the PGC-1$\alpha^{-/-}\beta^{f/f/MLC\text{-}Cre}$ muscle. For these studies, activity of the mitochondrial enzyme succinate dehydrogenase (SDH) was used

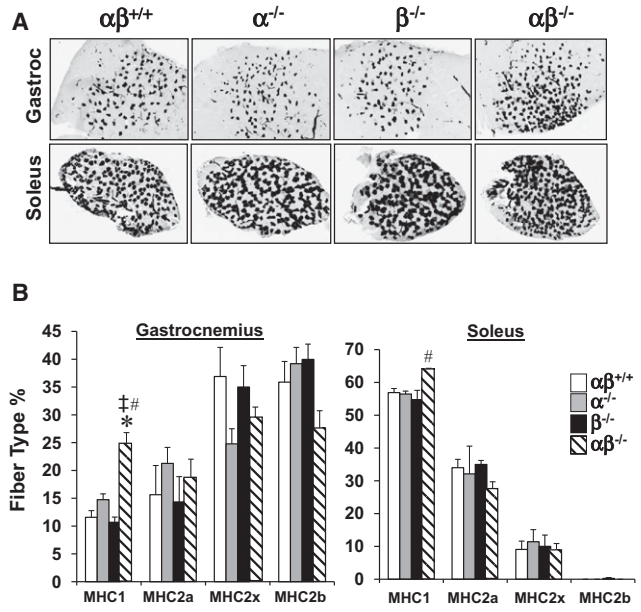

Figure 3. PGC-1$\alpha^{-/-}\beta^{f/f/MCK\text{-}Cre}$ Muscle Exhibits a Mild Increase in MHC1-Positive Fibers without a Change in Type II Fiber Formation

(A) Representative sections of GC and soleus muscle from PGC-1$\alpha^{-/-}\beta^{f/f/MCK\text{-}Cre}$ mice (see also Figure S3) stained for myosin ATPase activity.

(B) Quantification of IHC immunostaining studies expressed as mean percent (± SEM) of total muscle fibers (n = 3–5/group). *p < 0.05 versus $\alpha\beta^{+/+}$; ‡p < 0.05 versus $\alpha^{-/-}$; #p < 0.05 versus $\beta^{-/-}$.

as an endpoint. SDH activity staining was only minimally reduced in PGC-1$\alpha^{-/-}\beta^{f/f}$ and PGC-1$\beta^{f/f/MLC\text{-}Cre}$ GC and soleus muscle compared to PGC-1$\beta^{f/f}$ controls (Figure 2C). In striking contrast, SDH staining was dramatically reduced in PGC-1$\alpha^{-/-}\beta^{f/f/MLC\text{-}Cre}$ muscle (Figure 2C). Thus, PGC-1 coactivators are required to maintain skeletal muscle oxidative capacity but not fiber type determination.

The fiber typing studies described above only allowed us to explore the effects of PGC-1α/PGC-1β deficiency in type II fibers given the fiber specificity of MLC1f-Cre. To assess the effects of combined PGC-1α/PGC-1β deficiency on type I fibers, PGC-1$\alpha^{-/-}\beta^{f/f}$ mice were bred with mice expressing a muscle creatine kinase (MCK) promoter-driven Cre (MCK-Cre) to establish the PGC-1$\alpha^{-/-}\beta^{f/f/MCK\text{-}Cre}$ line, in which the *PGC-1β* gene is disrupted in both fast- and slow-twitch muscle fiber types in a PGC-1α-deficient background. As expected, expression of the *PGC-1β* gene was significantly reduced in fast and slow muscles in PGC-1$\alpha^{-/-}\beta^{f/f/MCK\text{-}Cre}$ mice (Figure S3). As we found for the PGC-1$\beta^{f/f/MLC\text{-}Cre}$ mice, PGC-1α mRNA levels were unchanged in the muscle of the PGC-1$\beta^{f/f/MCK\text{-}Cre}$ mice (data not shown). The PGC-1$\alpha^{-/-}\beta^{f/f/MCK\text{-}Cre}$ line also had significant reduction in cardiac PGC-1β expression, which resulted in cardiomyopathy by 1 month of age (data not shown), a finding that was predicted, given that cardiac PGC-1α/PGC-1β deficiency causes postnatal heart failure (Lai et al., 2008). As observed in PGC-1$\alpha^{-/-}\beta^{f/f/MLC\text{-}Cre}$ muscle, type I fiber type proportion was slightly increased without changes in the relative proportions of the other fiber types in PGC-1$\alpha^{-/-}\beta^{f/f/MCK\text{-}Cre}$ mice, based on metachromatic staining and MHC immunohistochemistry performed on soleus and GC sections (Figures 3A and 3B). Together with the results obtained from the PGC-1$\alpha^{-/-}\beta^{f/f/MLC\text{-}Cre}$ mice, these data strongly suggest that PGC-1α and PGC-1β are dispensable for skeletal muscle development and fundamental fiber type determination.

Mitochondrial Structural and Functional Derangements in PGC-1$\alpha^{-/-}\beta^{f/f/MLC\text{-}Cre}$ Muscle

Transcriptional profiling studies were conducted using GC to gain further insight into the alterations in PGC-1$\alpha^{-/-}\beta^{f/f/MLC\text{-}Cre}$ muscle. We were particularly interested in the subset of genes that were downregulated only in the doubly deficient mice. The number of genes (array probes) that were downregulated uniquely or shared by the three genotypes is displayed in the Venn diagram (Figure 4A). Of the 5526 genes that were downregulated in the PGC-1$\alpha^{-/-}\beta^{f/f/MLC\text{-}Cre}$, 2839 were uniquely downregulated compared to the other two genotypes. In addition, 1086 genes were upregulated in PGC-1$\alpha^{-/-}\beta^{f/f/MLC\text{-}Cre}$ muscle (data not shown).

Gene ontology (GO) analysis demonstrated that mitochondrial pathways were rarely downregulated in singly PGC-1α- or PGC-1β-deficient muscle (4/229 or 1.7% of total pathways). In contrast, 47/202 (or 23%) of total pathways downregulated only in the double knockout muscle were involved in mitochondrial processes, including the TCA cycle, electron transport, OXPHOS, and mitochondrial membrane organization and biogenesis (Table S1, shaded pathways). Only two pathways were significantly upregulated in the double knockout, neither of which was mitochondrial. Quantitative RT-PCR validation studies were conducted on a subset of genes representative of the latter pathways (identified as uniquely downregulated in the PGC-1$\alpha^{-/-}\beta^{f/f/MLC\text{-}Cre}$ muscle). Levels of mRNA-encoding enzymes involved in the TCA cycle (citrate synthase [Cs]), electron transport chain/OXPHOS (cytochrome oxidase subunit IV isoform 1 [Cox4i1] and ATP synthase F1 complex beta subunit [ATP5b]), mitochondrial membrane transport (adenine nucleotide translocator 1 [Ant1]), and reactive oxygen species scavenging (mitochondrial superoxide dismutase 2 [Sod2]) were downregulated in PGC-1$\alpha^{-/-}\beta^{f/f}$ muscle (and some in PGC-1$\beta^{f/f/MLC\text{-}Cre}$) and further reduced in PGC-1$\alpha^{-/-}\beta^{f/f/MLC\text{-}Cre}$ muscle when compared to PGC-1$\beta^{f/f}$ controls (Figure 4B). However, levels of mRNA encoding other enzymes, such as those involved in fatty acid oxidation (carnitine palmitoyltransferase 1b [Cpt1b] and medium-chain acyl-coenzyme A dehydrogenase [Acadm]), was reduced in PGC-1$\alpha^{-/-}\beta^{f/f}$ muscle, but not further downregulated in the double knockout muscle. Interestingly, expression of the gene encoding nuclear respiratory factor 1 (NRF-1), a PGC-1α target (Wu et al., 1999) involved in regulating OXPHOS genes and coordinating nuclear and mitochondrial genomes, was similar among the groups. This latter result is consistent with the findings of a previous study showing no effect of loss of PGC-1α on NRF-1 expression in the heart (Arany et al., 2005) or skeletal muscle (Geng et al., 2010). Taken together, the transcriptional profiling results indicate that a significant subset of PGC-1 target genes, particularly those involved in mitochondrial energy transduction pathways, are shared by the PGC-1 coactivators. It should also be noted that within the shared target gene data set, loss of PGC-1α alone often had a greater impact than PGC-1β deficiency (Figure 4B).

Further review of the gene expression array data revealed that several genes involved in mitochondrial dynamics,

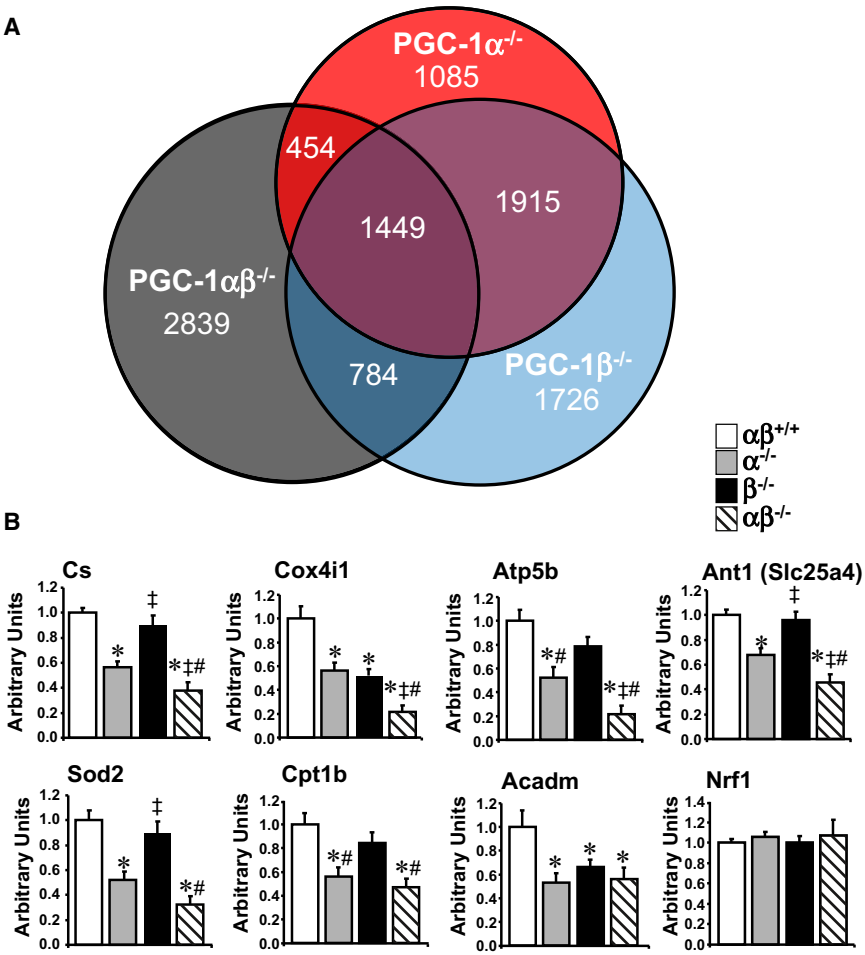

Figure 4. PGC-1α and β Drive an Overlapping Subset of Target Genes Involved in Mitochondrial Processes

(A) Venn diagram displaying the results of gene expression microarray analysis conducted on RNA isolated from PGC-1$\alpha^{-/-}\beta^{f/f}$ ($\alpha^{-/-}$), PGC-1$\beta^{f/f/MLC\text{-}Cre}$ ($\beta^{-/-}$), and PGC-1$\alpha^{-/-}\beta^{f/f/MLC\text{-}Cre}$ ($\alpha\beta^{-/-}$) GC muscle compared to PGC-1$\beta^{f/f}$ controls. The numbers denote number of downregulated gene probes ($\leq$0.7) in the corresponding sector.

(B) Levels of mRNAs based on quantitative real-time RT-PCR performed on RNA isolated from GC muscle of 3- to 4-month-old male mice from the genotypes indicated (n = 8–10 per group). Citrate synthase, Cs; cytochrome *c* oxidase subunit 4 isoform 1, Cox4i1; beta polypeptide of the H^+ transporting mitochondrial F1 complex ATP synthase, Atp5b; adenine nucleotide translocator 1, Ant1 = Slc25a4; mitochondrial superoxide dismutase 2, Sod2; the muscle isoform of carnitine-palmitoyl transferase 1, Cpt1b; medium chain acyl-CoA dehydrogenase, Acadm; and nuclear respiratory factor 1, Nrf1. Bars represent mean values (± SEM) normalized to 36B4 mRNA levels and expressed relative (= 1.0) to PGC-1$\beta^{f/f}$ ($\alpha\beta^{+/+}$) muscle. *p < 0.05 versus $\alpha\beta^{+/+}$; ‡p < 0.05 versus $\alpha^{-/-}$; #p < 0.05 versus $\beta^{-/-}$.

including fusion and fission, were also downregulated in PGC-1$\alpha^{-/-}\beta^{f/f/MLC\text{-}Cre}$ muscle (GO ID 7006, 5741, 5743, 31966) (Table S1). Validation studies confirmed that the expression of mitofusin (*Mfn*) 1 and 2 genes and the gene encoding dynamin-related protein 1 (*Drp1*, *dnm1l*), a key mitochondrial fission protein, was significantly downregulated in the muscle of the PGC-1$\alpha^{-/-}\beta^{f/f/MLC\text{-}Cre}$ mice compared to the other groups (Figure 5A). These results suggested that the PGC-1 coactivators are necessary for mitochondrial dynamics and quality control in skeletal muscle. Therefore, mitochondrial volume density, size, and ultrastructure were assessed by electron microscopy in the intermyofibrillar (IM) and subsarcolemmal (SS) compartments of the GC muscle fibers of all four genotypes. This analysis revealed striking mitochondrial morphologic abnormalities in IM and SS regions in the PGC-1$\alpha^{-/-}\beta^{f/f/MLC\text{-}Cre}$ muscle compared to the other genotypes, including a reduction in density and heterogeneity of size (Figure 5B and data not shown). The muscle mitochondria of PGC-1$\alpha^{-/-}\beta^{f/f/MLC\text{-}Cre}$ mice contained many small, fragmented mitochondria juxtaposed to elongated, thin mitochondria (arrows, Figure 5B). Mitochondrial DNA levels were reduced in parallel with the observed ultrastructural derangements among the genotypes (Figure S4). Taken together, these results implicate the PGC-1 coactivators in muscle mitochondrial biogenesis and fusion/fission programs.

Respiration rates were determined on mitochondria isolated from the hindlimb of all four genotypes using pyruvate or palmitoylcarnitine as substrates. Consistent with the dramatic structural derangements, state 3 respiration rates were markedly reduced in PGC-1$\alpha^{-/-}\beta^{f/f/MLC\text{-}Cre}$ muscle compared to the WT controls (Figure 5C). State 3 rates in mitochondria from single PGC-1 gene-deficient muscle were reduced to a level midway between the WT controls and that of PGC-1$\alpha^{-/-}\beta^{f/f/MLC\text{-}Cre}$ mice (Figure 5C).

Muscle PGC-1α/β Deficiency Does Not Affect Glucose Tolerance or Insulin Resistance

We next sought to assess glucose utilization and insulin responsiveness in the PGC-1$\alpha^{-/-}\beta^{f/f/MLC\text{-}Cre}$ mice. Mice of all four genotypes were subjected to glucose tolerance (GTT) and insulin tolerance (ITT) testing. For initial studies on standard chow, we compared results obtained with PGC-1$\beta^{f/f}$ and PGC-1$\beta^{f/f/MLC\text{-}Cre}$ or PGC-1$\alpha^{-/-}\beta^{f/f}$ and PGC-1$\alpha^{-/-}\beta^{f/f/MLC\text{-}Cre}$ so that littermate comparisons were possible. Neither the muscle-specific PGC-1β-deficient (PGC-1$\beta^{f/f/MLC\text{-}Cre}$) (Figure 6A) nor the double knockout (PGC-1$\alpha^{-/-}\beta^{f/f/MLC\text{-}Cre}$) (Figure 6B) line exhibited glucose intolerance or insulin resistance when compared with their respective controls. The studies were then repeated after an 8 week high-fat-diet regimen to determine whether this intervention would unveil a phenotype. As with standard diet, there was no difference in ITT or GTT among the genotypes on the high-fat diet (Figure 6C). In addition, fasting levels of glucose, insulin, free fatty acids, and triglycerides were not different among the groups (Figure S5). Skeletal muscle

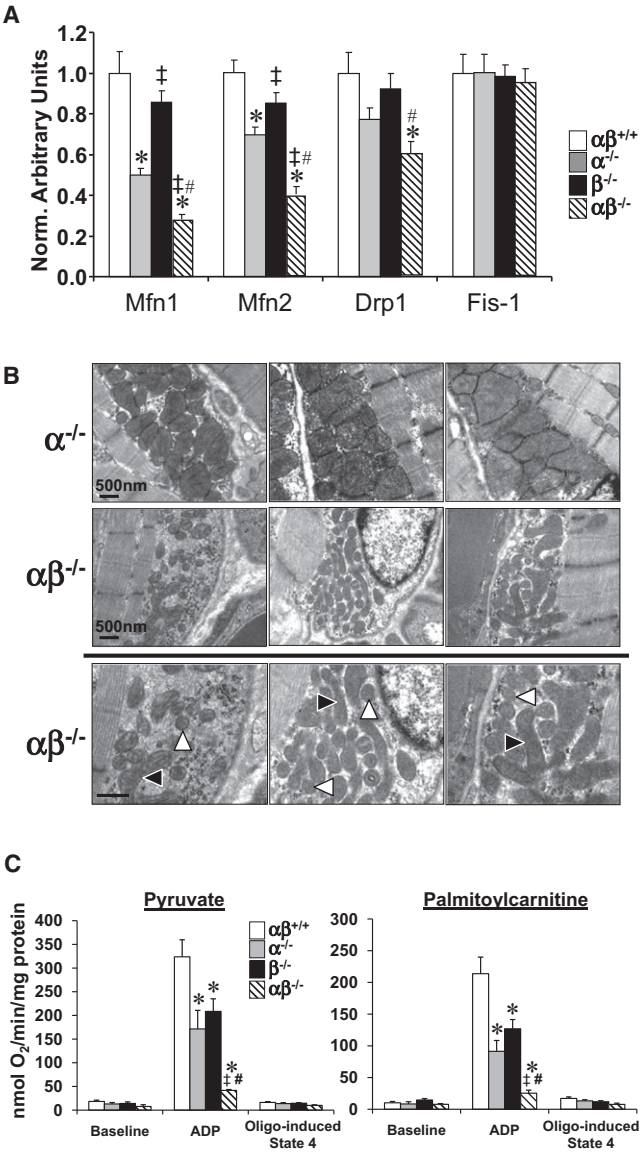

Figure 5. PGC-1$\alpha^{-/-}\beta^{f/f/MLC\text{-}Cre}$ Muscle Exhibits Mitochondrial Structural and Functional Abnormalities and Dysregulation of Genes Involved in Mitochondrial Dynamics

(A) Levels of mRNAs encoding mitochondrial fission and fusion genes, including mitofusin 1 (*Mfn1*), mitofusin 2 (*Mfn2*), dynamin-related protein 1 (*Drp1* or *dmn1l*), and mitochondrial outer membrane fission 1 homolog (yeast) (*Fis-1*), determined by quantitative real-time RT-PCR (n = 7–8 per group). Bars represent mean values (± SEM) normalized to 36B4 mRNA levels and expressed relative (= 1.0) to PGC-1$\beta^{f/f}$ ($\alpha\beta^{+/+}$) muscle.

(B) Representative electron micrographs of gastrocnemius showing subsarcolemmal mitochondria in sections from PGC-1$\alpha^{-/-}\beta^{f/f}$ mice ($\alpha^{-/-}$; top row) and PGC-1$\alpha^{-/-}\beta^{f/f/MLC\text{-}Cre}$ mice (middle row and magnified in bottom row). Note small, fragmented (white arrowhead), and elongated (black arrowhead) mitochondria. Scale bars represent 500 nm.

(C) Bars represent mean (± SEM) mitochondrial respiration rates determined on mitochondria isolated from the entire hindlimb muscle of the four genotypes shown using pyruvate or palmitoylcarnitine as a substrate (4–6 male animals per group). Rates were measured under the following conditions: basal, state 3 (ADP-stimulated), and after oligomycin treatment (oligo-induced State 4). *p < 0.05 versus $\alpha\beta^{+/+}$; ‡p < 0.05 versus $\alpha^{-/-}$; #p < 0.05 versus $\beta^{-/-}$. See also Figure S4.

triglyceride levels were also similar among the four genotypes (Figure S5).

To further evaluate muscle glucose utilization in the PGC-1$\alpha^{-/-}\beta^{f/f/MLC\text{-}Cre}$ mice, glycogen levels were assessed pre- and postexercise. For these experiments, the four genotype groups were run for a duration matched to the time required for the PGC-1$\alpha^{-/-}\beta^{f/f/MLC\text{-}Cre}$ mice to reach exhaustion. Baseline glycogen levels in the GC did not differ between groups. The bout of exercise rapidly depleted stores in PGC-1$\alpha^{-/-}\beta^{f/f/MLC\text{-}Cre}$ mice but did not significantly change muscle glycogen levels in the PGC-1$\beta^{f/f}$, PGC-1$\alpha^{-/-}\beta^{f/f}$, and PGC-1$\beta^{f/f/MLC\text{-}Cre}$ groups (Figure 7A). These results suggested that the PGC-1$\alpha^{-/-}\beta^{f/f/MLC\text{-}Cre}$ muscle relies largely on anaerobic glycolysis for ATP production during exercise. This conclusion is supported by the observation that blood lactate levels increased markedly in the PGC-1$\alpha^{-/-}\beta^{f/f/MLC\text{-}Cre}$ mice following a bout of exhaustive exercise compared to that of WT and PGC-1$\beta^{f/f/MLC\text{-}Cre}$ after exhaustive exercise (Figure 7B). Blood lactate levels also increased in the PGC-1$\alpha^{-/-}\beta^{f/f}$ mice, but to a lesser extent than the PGC-1$\alpha^{-/-}\beta^{f/f/MLC\text{-}Cre}$ group. These results are consistent with the observation of normal glucose tolerance and help explain the severe exercise deficit, given that glucose derived from glycogen serves as an obligate fuel source during exercise.

DISCUSSION

We devised a strategy to disrupt the *PGC-1β* gene in a skeletal-muscle-selective manner in a generalized PGC-1α-deficient mouse background. As described herein, we found that PGC-1α and PGC-1β serve overlapping roles in skeletal muscle and together are necessary for exercise performance (even minimal exertion) and maintenance of mitochondrial structure and function, but are dispensable for fundamental fiber type determination and normal muscle insulin sensitivity and glucose disposal.

Our findings demonstrated that the cooperative and overlapping actions of PGC-1α and PGC-1β are required for muscle mitochondrial function and structure. Transcriptional profiling studies revealed that the expression of a broad array of genes involved in multiple mitochondrial energy transduction and OXPHOS pathways is dependent on having at least one functional PGC-1 gene. PGC-1α/β deficiency resulted in dramatic derangements in mitochondrial structure and respiratory function, indicating that the PGC-1 coactivators are required for maintaining a healthy population of normal mitochondria. This latter function has been ascribed to the ongoing dynamics of fusion and fission, which serve to maintain mitochondrial quality control (Chen et al., 2005; Waterham et al., 2007; Zhang and Chan, 2007). Consistent with this conclusion, we found that the expression of genes involved in fusion (*Mfn1*, *Mfn2*) and fission (*Drp1*) was downregulated in the muscle of PGC-1$\alpha^{-/-}\beta^{f/f/MLC\text{-}Cre}$ mice compared to the other genotypes. Others have recently shown that PGC-1α and PGC-1β are capable of activating transcription of the *Mfn2* gene by coactivating the nuclear receptor ERRα (Soriano et al., 2006; Liesa et al., 2008). Taken together, these results suggest that the PGC-1 coactivators are necessary for maintaining high-level coordinated expression of genes involved in mitochondrial energy transduction and ATP production pathways, as well as maintenance of a healthy population of muscle mitochondria.

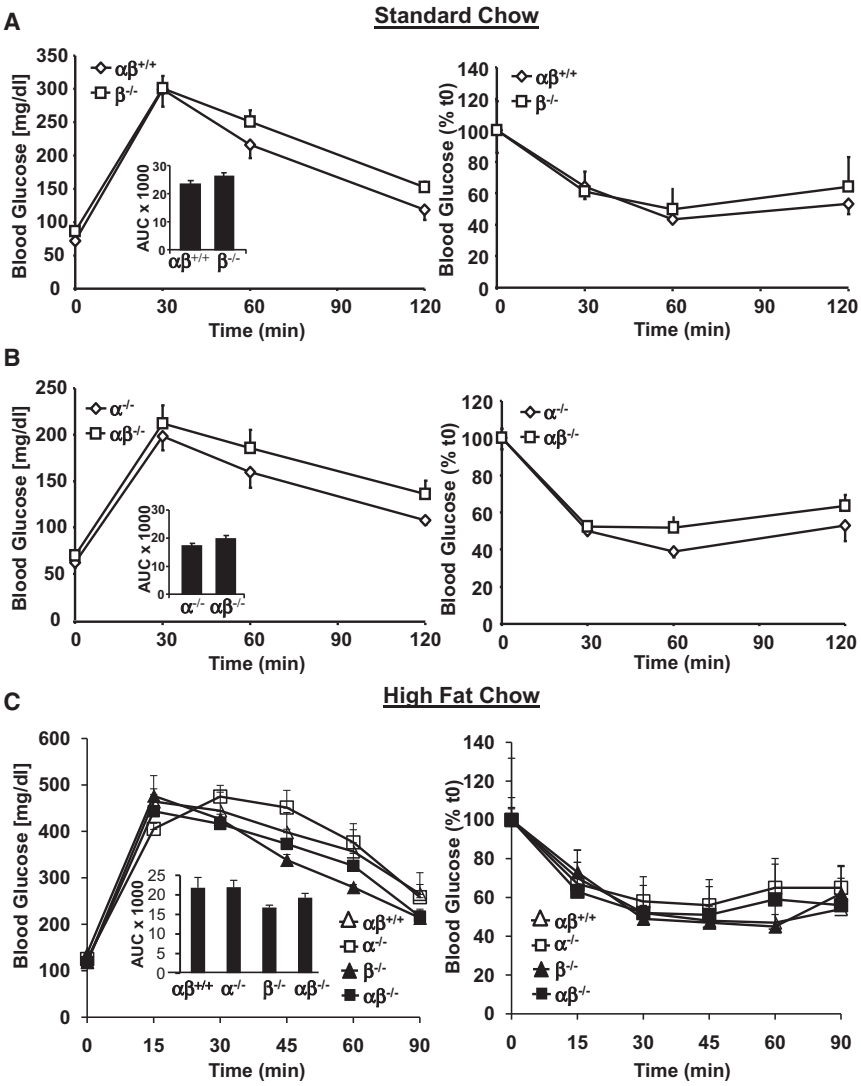

Figure 6. Global Loss of PGC-1α Combined with Muscle-Specific Loss of PGC-1β Does Not Result in Glucose Intolerance or Insulin Resistance

(A) Mean blood glucose (± SEM) levels during GTT (left) and ITT (right) using 2- to 3-month-old male littermate PGC-1$\beta^{f/f}$ ($\alpha\beta^{+/+}$) and PGC-1$\beta^{f/f/MLC\text{-}Cre}$ ($\beta^{-/-}$) mice on standard chow as described in the Experimental Procedures (n = 9–10). Total area under the glucose excursion curve (± SEM) is displayed in the inset for the GTT.

(B) GTT and ITT results (mean blood glucose ± SEM) for 2- to 3-month-old male littermate PGC-1$\alpha^{-/-}\beta^{f/f}$ ($\alpha^{-/-}$) and PGC-1$\alpha^{-/-}\beta^{f/f/MLC\text{-}Cre}$ ($\alpha\beta^{-/-}$) mice on standard chow (n = 11–13 per group).

(C) Results of GTT (left) and ITT (right), expressed as mean blood glucose ± SEM, conducted on 13-week-old male mice after 8 weeks of high-fat diet (n = 3–6/group). See also Figure S5.

The impact of combined PGC-1α and PGC-1β deficiency on exercise performance was dramatic. Our results strongly suggest that the exercise phenotype is due to severe mitochondrial dysfunction forcing reliance on anaerobic glycolysis for ATP production, leading to rapid depletion of glycogen and premature fatigue. The marked elevation in circulating lactate levels in the PGC-1α/β-deficient mice postexercise is consistent with this conclusion. Interestingly, lactate levels were also increased postexercise in the PGC-1$\alpha^{-/-}$ mice, albeit to a lesser extent than the PGC-1α/β-deficient animals. This latter observation could reflect the fact that hepatic PGC-1α deficiency results in an altered Cori cycle response. It is also possible that PGC-1 coactivators play a primary role in glycogen metabolism. However, the protein levels of the enzymes involved in glycogen synthesis and degradation were not significantly altered in the PGC-1$\alpha^{-/-}\beta^{f/f/MLC\text{-}Cre}$ mice (data not shown).

Surprisingly, combined PGC-1α/β deficiency results in a remarkable uncoupling of muscle fiber type and oxidative programs. Specifically, phenotypic analysis of the PGC-1$\alpha^{-/-}\beta^{f/f/MLC\text{-}Cre}$ mice did not reveal a shift toward a "detrained" muscle fiber type profile, as would be predicted by PGC-1 overexpression studies. Rather, we found a modest increase in type I fibers in the muscles of both PGC-1$\alpha^{-/-}\beta^{f/f/MLC\text{-}Cre}$ and PGC-1$\alpha^{-/-}\beta^{f/f/MCK\text{-}Cre}$ lines. The observed increase in type I fibers in the mutant mice suggests that an independent, currently unidentified pathway involved in fundamental fiber type is compensatorily activated. PGC-1 overexpression in mice has been shown to inhibit the protein degradation known to occur in disuse atrophy (Wenz et al., 2009; Brault et al., 2010). However, we did not find an overt abnormality in muscle mass in the PGC-1$\alpha^{-/-}\beta^{f/f/MLC\text{-}Cre}$ mice. Thus, whereas PGC-1 coactivators are capable of driving a shift toward oxidative fibers and muscle growth, they are not required for fundamental muscle development or fiber type specification. One caveat to our conclusions is that a small amount of a mutant form of a naturally occurring, alternatively spliced form of PGC-1α, referred to as NT-PGC-1α (Zhang et al., 2009), could be theoretically expressed in the PGC-1α-deficient line used in this study. However, RT-PCR analysis demonstrated that levels of this transcript are barely detectable in muscle, as we have shown in the generalized PGC-1α-deficient line (Leone et al., 2005). Moreover, given the severe mitochondrial and exercise phenotype shown here, it would seem unlikely that this could account for a completely normal fiber phenotype.

Significant evidence suggests a link between skeletal muscle mitochondrial dysfunction and the development of insulin resistance (Lowell and Shulman, 2005; Morino et al., 2005; Petersen et al., 2005). In addition, several studies in humans have shown reduced expression of PGC-1α (Mootha et al., 2003; Patti et al., 2003) in skeletal muscle of insulin-resistant and diabetic subjects. These studies implicate muscle mitochondrial dysfunction and altered PGC-1 signaling in the pathogenesis

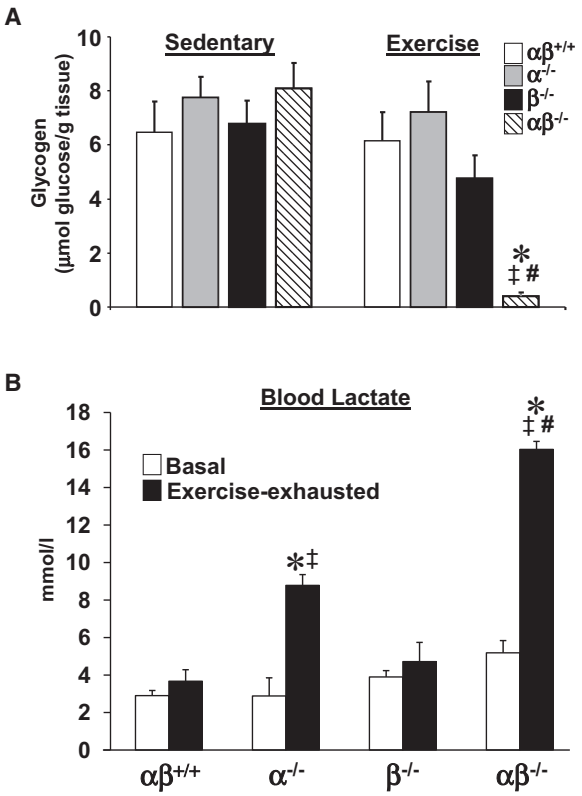

Figure 7. Combined Loss of Skeletal Muscle PGC-1α and β Results in Rapid Depletion of Muscle Glycogen during Exercise

(A) Mean glycogen levels (± SEM) of GC muscle of sedentary 2- to 3-month-old male mice of the indicated genotypes are shown on the left. The results of GC glycogen levels postexercise are shown on the right.

(B) Mean blood lactate levels (± SEM) at baseline (white bars) and following exhaustive exercise (black bars) for all four genotypes (n = 5–10/group). (Run-to-exhaustion protocol is described in text and Experimental Procedures.) *p < 0.05 versus $\alpha\beta^{+/+}$; ‡p < 0.05 versus $\alpha^{-/-}$; #p < 0.05 versus $\beta^{-/-}$.

of insulin resistance. The studies shown herein demonstrate that total skeletal muscle PGC-1 deficiency in mice does not lead to insulin resistance or glucose intolerance on standard chow or high-fat diet. Moreover, given the mitochondrial derangements present in PGC-1$\alpha^{-/-}\beta^{f/f/MLC\text{-}Cre}$ muscle, our results suggest that mitochondrial dysfunction is unlikely to contribute to insulin resistance. It is certainly possible, however, that insulin resistance drives muscle mitochondrial dysfunction.

EXPERIMENTAL PROCEDURES

Animal Studies

Generation of PGC-1$\beta^{f/f}$ mice has been described elsewhere (Lai et al., 2008). PGC-1$\beta^{f/f}$ mice were crossed with mice expressing Cre under control of a MLC1f promoter (Bothe et al., 2000) or the MCK promoter (Brüning et al., 1998) to achieve muscle-specific deletion of PGC-1β. These mice in turn were crossed to obtain mice homozygous for the loss of PGC-1α (Leone et al., 2005) and the PGC-1β flox allele (PGC-1$\alpha^{-/-}\beta^{f/f}$ mice), with and without MLC1f-Cre. (See Supplemental Experimental Procedures for more detail regarding the breeding strategy.)

Mice were maintained in the hybrid background, C57BL6/J x sv129, and littermate controls were used. PGC-1$\beta^{f/f}$ and PGC-1$\beta^{f/f/MLC\text{-}Cre}$ mice were generated from the same breeding pairs, while PGC-1$\alpha^{-/-}\beta^{f/f}$ and PGC-1$\alpha^{-/-}\beta^{f/f/MLC\text{-}Cre}$ mice were generated from a different set of breeding pairs. Male mice were used for all experiments unless otherwise stated.

Mice were allowed ad libitum access to standard laboratory rodent chow (diet 5053, Purina Mills Inc.) or high-fat diet (TD97268, Harlan Teklad) as indicated. All animal experiments and euthanasia protocols were conducted in strict accordance with the National Institutes of Health guidelines for humane treatment of animals and were reviewed and approved by the Institutional Animal Care and Use Committees of Washington University School of Medicine and the Sanford-Burnham Medical Research Institute.

Glucose and Insulin Tolerance Testing

Prior to studies, 2- to 3-month-old male mice on standard chow were fasted overnight (GTT) or for 6 hr (ITT). For GTT studies, mice were injected with 1 g/kg of D-glucose. For ITT, mice received an intraperitoneal injection of human regular insulin (Eli Lilly and Co.) at a dose of 0.75 U/kg body weight for ITT. The tip of the tail (~1 mm) was cut 60 min prior to the glucose or insulin challenge for blood sampling. Blood glucose levels were determined at several different time points after challenge using an Accu-Chek Advantage glucometer (Roche). For GTT, area under the curve (AUC) was defined as the difference between baseline glucose levels and the deflection caused by the glucose challenge. Total AUC was calculated using the trapezoidal rule. For the high-fat-diet study, mice were given high-fat diet beginning at 5 weeks of age. At 13 weeks of age, GTT and ITT were performed following a 5 hr fast. A dose of 2 g/kg D-glucose was used for the GTT.

Blood and Tissue Chemistry

After an 8 week high-fat-diet regimen, mice were fasted overnight (16 hr) beginning at 5 p.m. Blood samples (~1 ul) were obtained from the tail for measurement of blood glucose using an Accu-Chek Advantage glucometer (Roche). Additional blood (~50 ul) was obtained for insulin measurements. Plasma insulin levels were determined by ELISA (Mercodia, Inc.) following the manufacturer's instructions. Mice were euthanized by CO_2 inhalation after 10 weeks on high-fat diet, and plasma and tissue triglyceride concentrations were determined by colorimetric assays as previously described (Chen et al., 2008). Plasma free fatty acids were also determined by a colorimetric assay (Lin et al., 2002b).

Evaluation of Exercise Performance

Two- to three-month-old mice were run to exhaustion employing a motorized, speed-controlled, modular treadmill system (Columbus Instruments). The treadmill was equipped with an electric shock stimulus and an adjustable inclination angle. Running velocity was set to 10 m/min for 1 hr and increased by 2 m/min increments every 15 min. The inclination angle was level. Tail blood was taken before and immediately following the exhaustion point, and lactate levels were analyzed using a Lactate Pro blood lactate test meter (ARKRAY, Inc.). For the assessment of muscle glycogen and serum CK values, male PGC-1$\alpha^{-/-}\beta^{f/f/MLC\text{-}Cre}$ mice were run to exhaustion, and the exercise time of controls was matched to the running time of the respective PGC-1$\alpha^{-/-}\beta^{f/f/MLC\text{-}Cre}$ mouse. Mice used for glycogen measurements were euthanized immediately after the running bout while mice used for serum CK measurements were harvested 30 min after the exercise bout. For details on glycogen and CK measurements, see Supplemental Experimental Procedures.

Evaluation of Muscle Function and Locomotor Activity

Muscle strength, muscle use, and general activity levels were assessed in 3- to 4-month-old female mice. For the assessment of forelimb grip strength, a grip strength meter was used as previously described (Wozniak et al., 2007). (See Supplemental Experimental Procedures for more detail.)

RNA, DNA, and Protein Analysis

Quantitative real-time PCR was performed on total RNA as previously described (Huss et al., 2004). The mouse-specific primer-probe sets used to detect specific gene expression can be found in Table S2. 36B4 mRNA was measured in a separate well (in triplicate) and used to normalize the gene expression data.

Genomic/mitochondrial DNA was isolated using the RNAzol method, followed by back extraction with 4 M guanidine thiocyanate, 50 mM sodium

citrate, and 1 M Tris and an alcohol precipitation. Mitochondrial DNA content was determined by SYBR Green analysis (Applied Biosystems or Stratagene). The levels of NADH dehydrogenase subunit 1 (mitochondrial DNA) were normalized to the levels of lipoprotein lipase (genomic DNA). The primer sequences are noted in Table S2.

Gene Expression Profiling

The Digestive Diseases Research Core Center (DDRCC) Functional Genomics Core Facility at Washington University School of Medicine performed hybridization of total RNA from GC muscle of 12-week-old mice to Agilent G4122F Whole-Mouse Genome microarrays. Samples were hybridized in four experimental pairs (PGC-1$\alpha^{-/-}\beta^{f/f}$ versus PGC-1$\beta^{f/f}$, PGC-1$\beta^{f/f/MLC\text{-}Cre}$ versus PGC-1$\beta^{f/f}$, PGC-1$\alpha^{-/-}\beta^{f/f/MLC\text{-}Cre}$ versus PGC-1$\beta^{f/f}$, and PGC-1$\alpha^{-/-}\beta^{f/f/MLC\text{-}Cre}$ versus PGC-1$\alpha^{-/-}$) with three hybridizations per pair. See Supplemental Experimental Procedures for more detail.

Histology and Electron Microscopy

For electron microscopy (EM) analyses, adult mice were euthanized and muscle tissue was rapidly fixed with Karnovsky's fixative (2% glutaraldehyde, 1% paraformaldehyde, and 0.08% sodium cacodylate). Muscle was dissected and post-fixed in 1% osmium tetroxide, dehydrated in graded ethanol, embedded in Poly Bed plastic resin, and sectioned for EM. EM was performed by the Research Electron Microscopy Core at Washington University School of Medicine.

GC and soleus muscles were analyzed. Muscle tissue was formalin fixed and embedded in paraffin, sectioned, and stained with hematoxylin and eosin (H&E) and Masson's Trichrome. For SDH and MHC ATPase stains, muscle tissue was frozen down in isopentane that had been cooled in liquid nitrogen. SDH stains were performed as described previously (Wende et al., 2007). MHC ATPase stains were performed at pH 4.31. Under these acidic conditions, MHC2 isoforms are inactivated while MHC1 is still functional, resulting in addition of black dye to MHC1-positive muscle fibers. Muscles for MHC immunofluorescence (IF) analysis were embedded in OCT Compound (Tissue-Tek), and IF was performed as described previously (Waters et al., 2004). The fibers were quantified (MHC1, red; MHC2a, blue; MHC2x, black [unstained]; MHC2b, green), and results were expressed as relative numbers of the different fiber types.

Mitochondrial Respiration

Mitochondrial respiration was assessed in isolated mitochondria from the hindlimb muscle with pyruvate or palmitoylcarnitine as substrate, as described previously (Bhattacharya et al., 1991). (See Supplemental Experimental Procedures for more detail.)

Statistical Analysis

Data were analyzed using t tests or ANOVA where appropriate, with Newman-Keuls tests or pairwise comparisons (Bonferroni adjusted) used for post hoc analyses. The level of significance was set at $p < 0.05$ in all cases. Data are reported as mean values ± SEM.

ACCESSION NUMBERS

The data discussed in this publication, including tables denoting the genes significantly up- and downregulated in the PGC-1$\alpha^{-/-}\beta^{f/f/MLC\text{-}Cre}$ muscle, have been deposited in NCBI's Gene Expression Omnibus and are accessible through GEO Series accession number GSE23365 (http://www.ncbi.nlm.nih.gov/geo/query/acc.cgi?acc=GSE23365).

SUPPLEMENTAL INFORMATION

Supplemental Information includes Supplemental Experimental Procedures, five figures, and two tables and can be found with this article online at doi:10.1016/j.cmet.2010.11.008.

ACKNOWLEDGMENTS

This work was supported by NIH grants DK45416 and HL58427 (D.P.K.), Neuroscience Blueprint Interdisciplinary Core Grant P30 NS057105 (D.F.W.), an American Diabetes Association Research Award (AR050429, Z.Y.), Deutsche Forschungsgemeinschaft Research Fellowship ZE 796/2-1 (C.Z.), and the Digestive Diseases Research Center (P30 DK052574) at Washington University School of Medicine (WUSM). Special thanks to Genevieve DeMaria for assistance with manuscript preparation; Sara Conyers at WUSM for assistance with the behavioral studies; Jochen K. Lennerz at WUSM for helpful discussion regarding histology; Karen Green and William Kraft for performing the electron microscopy (WUSM Research Electron Microscopy Core Facility); Julio Ayala and Emily King of the Sanford-Burnham Cardiometabolic Phenotyping Core for assistance with GTT, ITT, and insulin measurements; and Suellen Greco (WUSM) for performing the CK measurements.

Received: May 28, 2010
Revised: August 19, 2010
Accepted: October 1, 2010
Published: November 30, 2010

REFERENCES

Arany, Z., He, H., Lin, J., Hoyer, K., Handschin, C., Toka, O., Ahmad, F., Matsui, T., Chin, S., Wu, P.H., et al. (2005). Transcriptional coactivator PGC-1 alpha controls the energy state and contractile function of cardiac muscle. Cell Metab. *1*, 259–271.

Arany, Z., Lebrasseur, N., Morris, C., Smith, E., Yang, W., Ma, Y., Chin, S., and Spiegelman, B.M. (2007). The transcriptional coactivator PGC-1beta drives the formation of oxidative type IIX fibers in skeletal muscle. Cell Metab. *5*, 35–46.

Baar, K., Wende, A.R., Jones, T.E., Marison, M., Nolte, L.A., Chen, M., Kelly, D.P., and Holloszy, J.O. (2002). Adaptations of skeletal muscle to exercise: rapid increase in the transcriptional coactivator PGC-1. FASEB J. *16*, 1879–1886.

Bhattacharya, S.K., Thakar, J.H., Johnson, P.L., and Shanklin, D.R. (1991). Isolation of skeletal muscle mitochondria from hamsters using an ionic medium containing ethylenediaminetetraacetic acid and nagarse. Anal. Biochem. *192*, 344–349.

Bothe, G.W., Haspel, J.A., Smith, C.L., Wiener, H.H., and Burden, S.J. (2000). Selective expression of Cre recombinase in skeletal muscle fibers. Genesis *26*, 165–166.

Brault, J.J., Jespersen, J.G., and Goldberg, A.L. (2010). Peroxisome proliferator-activated receptor gamma coactivator 1alpha or 1beta overexpression inhibits muscle protein degradation, induction of ubiquitin ligases, and disuse atrophy. J. Biol. Chem. *285*, 19460–19471.

Brüning, J.C., Michael, M.D., Winnay, J.N., Hayashi, T., Hörsch, D., Accili, D., Goodyear, L.J., and Kahn, C.R. (1998). A muscle-specific insulin receptor knockout exhibits features of the metabolic syndrome of NIDDM without altering glucose tolerance. Mol. Cell *2*, 559–569.

Chen, H., Chomyn, A., and Chan, D.C. (2005). Disruption of fusion results in mitochondrial heterogeneity and dysfunction. J. Biol. Chem. *280*, 26185–26192.

Chen, Z., Gropler, M.C., Norris, J., Lawrence, J.C., Jr., Harris, T.E., and Finck, B.N. (2008). Alterations in hepatic metabolism in fld mice reveal a role for lipin 1 in regulating VLDL-triacylglyceride secretion. Arterioscler. Thromb. Vasc. Biol. *28*, 1738–1744.

Donoghue, M.J., Alvarez, J.D., Merlie, J.P., and Sanes, J.R. (1991). Fiber type- and position-dependent expression of a myosin light chain-CAT transgene detected with a novel histochemical stain for CAT. J. Cell Biol. *115*, 423–434.

Finck, B.N., and Kelly, D.P. (2006). PGC-1 coactivators: inducible regulators of energy metabolism in health and disease. J. Clin. Invest. *116*, 615–622.

Geng, T., Li, P., Okutsu, M., Yin, X., Kwek, J., Zhang, M., and Yan, Z. (2010). PGC-1alpha plays a functional role in exercise-induced mitochondrial biogenesis and angiogenesis but not fiber-type transformation in mouse skeletal muscle. Am. J. Physiol. Cell Physiol. *298*, C572–C579.

Goto, M., Terada, S., Kato, M., Katoh, M., Yokozeki, T., Tabata, I., and Shimokawa, T. (2000). cDNA Cloning and mRNA analysis of PGC-1 in

epitrochlearis muscle in swimming-exercised rats. Biochem. Biophys. Res. Commun. *274*, 350–354.

Handschin, C., and Spiegelman, B.M. (2006). Peroxisome proliferator-activated receptor gamma coactivator 1 coactivators, energy homeostasis, and metabolism. Endocr. Rev. *27*, 728–735.

Handschin, C., Chin, S., Li, P., Liu, F., Maratos-Flier, E., Lebrasseur, N.K., Yan, Z., and Spiegelman, B.M. (2007). Skeletal muscle fiber-type switching, exercise intolerance, and myopathy in PGC-1alpha muscle-specific knock-out animals. J. Biol. Chem. *282*, 30014–30021.

Huss, J.M., Torra, I.P., Staels, B., Giguère, V., and Kelly, D.P. (2004). Estrogen-related receptor alpha directs peroxisome proliferator-activated receptor alpha signaling in the transcriptional control of energy metabolism in cardiac and skeletal muscle. Mol. Cell. Biol. *24*, 9079–9091.

Kelly, D.P., and Scarpulla, R.C. (2004). Transcriptional regulatory circuits controlling mitochondrial biogenesis and function. Genes Dev. *18*, 357–368.

Lai, L., Leone, T.C., Zechner, C., Schaeffer, P.J., Kelly, S.M., Flanagan, D.P., Medeiros, D.M., Kovacs, A., and Kelly, D.P. (2008). Transcriptional coactivators PGC-1alpha and PGC-lbeta control overlapping programs required for perinatal maturation of the heart. Genes Dev. *22*, 1948–1961.

Lehman, J.J., Barger, P.M., Kovacs, A., Saffitz, J.E., Medeiros, D.M., and Kelly, D.P. (2000). Peroxisome proliferator-activated receptor gamma coactivator-1 promotes cardiac mitochondrial biogenesis. J. Clin. Invest. *106*, 847–856.

Lelliott, C.J., Medina-Gomez, G., Petrovic, N., Kis, A., Feldmann, H.M., Bjursell, M., Parker, N., Curtis, K., Campbell, M., Hu, P., et al. (2006). Ablation of PGC-1beta results in defective mitochondrial activity, thermogenesis, hepatic function, and cardiac performance. PLoS Biol. *4*, e369.

Leone, T.C., Lehman, J.J., Finck, B.N., Schaeffer, P.J., Wende, A.R., Boudina, S., Courtois, M., Wozniak, D.F., Sambandam, N., Bernal-Mizrachi, C., et al. (2005). PGC-1alpha deficiency causes multi-system energy metabolic derangements: muscle dysfunction, abnormal weight control and hepatic steatosis. PLoS Biol. *3*, e101.

Liesa, M., Borda-d'Agua, B., Medina-Gómez, G., Lelliott, C.J., Paz, J.C., Rojo, M., Palacín, M., Vidal-Puig, A., and Zorzano, A. (2008). Mitochondrial fusion is increased by the nuclear coactivator PGC-1beta. PLoS ONE *3*, e3613.

Lin, J., Wu, H., Tarr, P.T., Zhang, C.Y., Wu, Z., Boss, O., Michael, L.F., Puigserver, P., Isotani, E., Olson, E.N., et al. (2002a). Transcriptional co-activator PGC-1 alpha drives the formation of slow-twitch muscle fibres. Nature *418*, 797–801.

Lin, X., Schonfeld, G., Yue, P., and Chen, Z. (2002b). Hepatic fatty acid synthesis is suppressed in mice with fatty livers due to targeted apolipoprotein B38.9 mutation. Arterioscler. Thromb. Vasc. Biol. *22*, 476–482.

Lin, J., Wu, P.H., Tarr, P.T., Lindenberg, K.S., St-Pierre, J., Zhang, C.Y., Mootha, V.K., Jäger, S., Vianna, C.R., Reznick, R.M., et al. (2004). Defects in adaptive energy metabolism with CNS-linked hyperactivity in PGC-1alpha null mice. Cell *119*, 121–135.

Lin, J., Handschin, C., and Spiegelman, B.M. (2005). Metabolic control through the PGC-1 family of transcription coactivators. Cell Metab. *1*, 361–370.

Lowell, B.B., and Shulman, G.I. (2005). Mitochondrial dysfunction and type 2 diabetes. Science *307*, 384–387.

Mootha, V.K., Lindgren, C.M., Eriksson, K.F., Subramanian, A., Sihag, S., Lehar, J., Puigserver, P., Carlsson, E., Ridderstråle, M., Laurila, E., et al. (2003). PGC-1alpha-responsive genes involved in oxidative phosphorylation are coordinately downregulated in human diabetes. Nat. Genet. *34*, 267–273.

Morino, K., Petersen, K.F., Dufour, S., Befroy, D., Frattini, J., Shatzkes, N., Neschen, S., White, M.F., Bilz, S., Sono, S., et al. (2005). Reduced mitochondrial density and increased IRS-1 serine phosphorylation in muscle of insulin-resistant offspring of type 2 diabetic parents. J. Clin. Invest. *115*, 3587–3593.

Parsons, S.A., Millay, D.P., Wilkins, B.J., Bueno, O.F., Tsika, G.L., Neilson, J.R., Liberatore, C.M., Yutzey, K.E., Crabtree, G.R., Tsika, R.W., and Molkentin, J.D. (2004). Genetic loss of calcineurin blocks mechanical overload-induced skeletal muscle fiber type switching but not hypertrophy. J. Biol. Chem. *279*, 26192–26200.

Patti, M.E., Butte, A.J., Crunkhorn, S., Cusi, K., Berria, R., Kashyap, S., Miyazaki, Y., Kohane, I., Costello, M., Saccone, R., et al. (2003). Coordinated reduction of genes of oxidative metabolism in humans with insulin resistance and diabetes: Potential role of PGC1 and NRF1. Proc. Natl. Acad. Sci. USA *100*, 8466–8471.

Petersen, K.F., Dufour, S., and Shulman, G.I. (2005). Decreased insulin-stimulated ATP synthesis and phosphate transport in muscle of insulin-resistant offspring of type 2 diabetic parents. PLoS Med. *2*, e233.

Pilegaard, H., Saltin, B., and Neufer, P.D. (2003). Exercise induces transient transcriptional activation of the PGC-1alpha gene in human skeletal muscle. J. Physiol. *546*, 851–858.

Puigserver, P., Wu, Z., Park, C.W., Graves, R., Wright, M., and Spiegelman, B.M. (1998). A cold-inducible coactivator of nuclear receptors linked to adaptive thermogenesis. Cell *92*, 829–839.

Sonoda, J., Mehl, I.R., Chong, L.W., Nofsinger, R.R., and Evans, R.M. (2007). PGC-1beta controls mitochondrial metabolism to modulate circadian activity, adaptive thermogenesis, and hepatic steatosis. Proc. Natl. Acad. Sci. USA *104*, 5223–5228.

Soriano, F.X., Liesa, M., Bach, D., Chan, D.C., Palacín, M., and Zorzano, A. (2006). Evidence for a mitochondrial regulatory pathway defined by peroxisome proliferator-activated receptor-gamma coactivator-1 alpha, estrogen-related receptor-alpha, and mitofusin 2. Diabetes *55*, 1783–1791.

Vianna, C.R., Huntgeburth, M., Coppari, R., Choi, C.S., Lin, J., Krauss, S., Barbatelli, G., Tzameli, I., Kim, Y.B., Cinti, S., et al. (2006). Hypomorphic mutation of PGC-1beta causes mitochondrial dysfunction and liver insulin resistance. Cell Metab. *4*, 453–464.

Waterham, H.R., Koster, J., van Roermund, C.W., Mooyer, P.A., Wanders, R.J., and Leonard, J.V. (2007). A lethal defect of mitochondrial and peroxisomal fission. N. Engl. J. Med. *356*, 1736–1741.

Waters, R.E., Rotevatn, S., Li, P., Annex, B.H., and Yan, Z. (2004). Voluntary running induces fiber type-specific angiogenesis in mouse skeletal muscle. Am. J. Physiol. Cell Physiol. *287*, C1342–C1348.

Wende, A.R., Schaeffer, P.J., Parker, G.J., Zechner, C., Han, D.H., Chen, M.M., Hancock, C.R., Lehman, J.J., Huss, J.M., McClain, D.A., et al. (2007). A role for the transcriptional coactivator PGC-1alpha in muscle refueling. J. Biol. Chem. *282*, 36642–36651.

Wenz, T., Rossi, S.G., Rotundo, R.L., Spiegelman, B.M., and Moraes, C.T. (2009). Increased muscle PGC-1alpha expression protects from sarcopenia and metabolic disease during aging. Proc. Natl. Acad. Sci. USA *106*, 20405–20410.

Wozniak, D.F., Xiao, M., Xu, L., Yamada, K.A., and Ornitz, D.M. (2007). Impaired spatial learning and defective theta burst induced LTP in mice lacking fibroblast growth factor 14. Neurobiol. Dis. *26*, 14–26.

Wu, Z., Puigserver, P., Andersson, U., Zhang, C., Adelmant, G., Mootha, V., Troy, A., Cinti, S., Lowell, B., Scarpulla, R.C., and Spiegelman, B.M. (1999). Mechanisms controlling mitochondrial biogenesis and respiration through the thermogenic coactivator PGC-1. Cell *98*, 115–124.

Zhang, Y., and Chan, D.C. (2007). Structural basis for recruitment of mitochondrial fission complexes by Fis1. Proc. Natl. Acad. Sci. USA *104*, 18526–18530.

Zhang, Y., Huypens, P., Adamson, A.W., Chang, J.S., Henagan, T.M., Boudreau, A., Lenard, N.R., Burk, D., Klein, J., Perwitz, N., et al. (2009). Alternative mRNA splicing produces a novel biologically active short isoform of PGC-1alpha. J. Biol. Chem. *284*, 32813–32826.